Biogeosciences, 5, 509–521, 2008
www.biogeosciences.net/5/509/2008/

Biogeosciences

Effects of CO_2 on particle size distribution and phytoplankton abundance during a mesocosm bloom experiment (PeECE II)

A. Engel[1], **K. G. Schulz**[2], **U. Riebesell**[2], **R. Bellerby**[3], **B. Delille**[4], **and M. Schartau**[5]

[1]Alfred Wegener Institute for Polar and Marine Research, Bremerhaven, Germany
[2]Leibniz Institute of Marine Sciences, IFM-GEOMAR, Kiel, Germany
[3]Bjerknes Centre for Climate Research, University of Bergen, Bergen, Norway
[4]Unité d'Océanographie Chimique, MARE, Université de Liège, Liège, Belgium
[5]Institute for Coastal Research, GKSS Research Centre, Geesthacht, Germany

Received: 19 October 2007 – Published in Biogeosciences Discuss.: 12 November 2007
Revised: 21 February 2008 – Accepted: 6 March 2008 – Published: 8 April 2008

Abstract. The influence of seawater carbon dioxide (CO_2) concentration on the size distribution of suspended particles (2–60 μm) and on phytoplankton abundance was investigated during a mesocosm experiment at the large scale facility (LFS) in Bergen, Norway, in the frame of the Pelagic Ecosystem CO_2 Enrichment study (PeECE II). In nine outdoor enclosures the partial pressure of CO_2 in seawater was modified by an aeration system to simulate past (~190 μatm CO_2), present (~370 μatm CO_2) and future (~700 μatm CO_2) CO_2 conditions in triplicates. Due to the initial addition of inorganic nutrients, phytoplankton blooms developed in all mesocosms and were monitored over a period of 19 days. Seawater samples were collected daily for analysing the abundance of suspended particles and phytoplankton with the Coulter Counter and with Flow Cytometry, respectively. During the bloom period, the abundance of small particles (<4 μm) significantly increased at past, and decreased at future CO_2 levels. At that time, a direct relationship between the total-surface-to-total-volume ratio of suspended particles and DIC concentration was determined for all mesocosms. Significant changes with respect to the CO_2 treatment were also observed in the phytoplankton community structure. While some populations such as diatoms seemed to be insensitive to the CO_2 treatment, others like *Micromonas spp*. increased with CO_2, or showed maximum abundance at present day CO_2 (i.e. *Emiliania huxleyi*). The strongest response to CO_2 was observed in the abundance of small autotrophic nano-plankton that strongly increased during the bloom in the past CO_2 mesocosms. Together, changes in particle size distribution and phytoplankton community indicate a complex interplay between the ability of the cells to physiologically respond to changes in CO_2 and size selection. Size of cells is of general importance for a variety of processes in marine systems such as diffusion-limited uptake of substrates, resource allocation, predator-prey interaction, and gravitational settling. The observed changes in particle size distribution are therefore discussed with respect to biogeochemical cycling and ecosystem functioning.

Correspondence to: A. Engel
(anja.engel@awi.de)

1 Introduction

The increase in atmospheric CO_2 concentration since the beginning of industrialisation, associated risks of ocean acidification, and the potential consequences for marine carbon cycling and global climate have recently gathered attention beyond purely scientific interest. Prior to the industrial burning of fossil fuels, CO_2 concentrations varied between 180 and 280 μatm, with the lower values observed during glacial times. Since the middle of the 18th century, the atmospheric concentration of CO_2 has increased rapidly from 280 μatm to 366 μatm in 1998, and several future scenarios predict a further increase to 750 μatm in 2100 (IPCC scenario IS92a) (Houghton et al., 2001). The seawater carbonate chemistry has responded noticeably, with a decrease from preindustrial surface ocean pH of 8.25 down to 8.08 presently. Modelling studies predict a further reduction of pH by 0.7 up to the year 2300, which would be more than experienced by marine life for the last 300 000 years (Caldeira and Wickett, 2003).

Although CO_2 plays a fundamental role for organic matter production in the ocean, as it is a substrate in algal photosynthesis, the direct effects of changes in CO_2 availability on organism performance, and their possible transfer to the

ecosystem level are still poorly understood. Only recently, studies showed that marine autotrophic communities such as seagrasses (Zimmerman et al., 1997), macroalgae (Gao et al., 1993), diatoms (Riebesell et al., 1993; Chen and Durbin, 1994), coccolithophores (Riebesell et al., 2000; Delille et al., 2005; Engel et al., 2005), and cyanobacteria (Qiu and Gao, 2002, Barcelos e Ramos et al., 2007; Hutchins et al., 2007) exhibit higher rates of production under CO_2 enrichment. It has also been shown that phytoplankton assemblages can experience marked shifts in composition under elevated pCO_2 conditions (Boyd and Doney, 2002; Tortell et al., 2002).

The previous reluctance to investigate direct effects of CO_2 on marine ecosystems largely resulted from the assumption that CO_2 is a non-limiting substrate for primary production in seawater. Although CO_2 concentrations in seawater range only between 8 and 22 μmol L^{-1} (Goerike and Fry, 1994), the total reservoir of dissolved inorganic carbon is about $\sim$2000 μmol L^{-1}. Thus, CO_2 is continuously supplied from the pool of bicarbonate and carbonate. Riebesell et al. (1993) showed that marine phytoplankton may indeed be limited by ambient CO_2 availability and respond to increased CO_2 concentration with increased growth rates. These results were somewhat contradictory to theoretical considerations, which indicated that for most phytoplankton cells the supply with CO_2 by diffusion is much larger than the cell's need for carbon (Wolf-Gladrow et al., 1999). Seemingly, it is the inefficiency of the CO_2/O_2 fixing enzyme Ribulose-1,5-bis-phosphate-carboxylase/oxygenase (RubisCo), with a half-saturation constant (Km) of 20–70 μmol L^{-1} (Badger et al., 1998), which causes a rate limitation of primary production in marine phytoplankton. However, measurements of primary production of various phytoplankton species revealed much lower Km values, indicating an enhanced CO_2 concentration at the site of carboxylation (Raven and Johnson, 1991; Rost et al., 2003; Giordano et al., 2005). Species with a low Km value have a high affinity to CO_2 and/or HCO_3^- and nearly saturate primary production at present day values, while at the same time minimizing energy loss due to photorespiration. An increase of seawater CO_2 must be anticipated to have little effect on primary production in these species. In contrast, for species with high Km, such as the coccolithophore *Emiliania huxleyi*, an enhancement of carboxylation can be expected, if CO_2 concentration increase from low values (6–8 μmol L^{-1}), as estimated for the last glacial maximum to high concentration as expected for the future ocean ($\sim$22 μmol L^{-1}) (Rost and Riebesell, 2004). Thus, under conditions where CO_2 concentration regulates growth (no co-limitation), species with high CO_2 affinity perform better and might out-compete those with lower affinity. The Km value for CO_2 depends, among others, on the capability of the phytoplankton cell to express carbon concentrating mechanisms (CCMs), which include active uptake of CO_2 and/or HCO_3^- and/ or enzymatically enhanced conversion of HCO_3^- to CO_2 (Raven and Johnson, 1991; Giordano et al., 2005). CCM operation has been observed in many marine microalgae, and we can expect selective advantages for those species that most efficiently apply CCMs to enhance carbon acquisition and cell growth. However, like any enzymatically driven process, CCMs require energy and substrates, in particular nitrogen, phosphate (ATP) and micronutrients for the synthesis and activation of involved enzymes, such as carbonic anhydrase (Young and Beardall, 2005; Beardall et al., 2005). Thus, the ability to express CCMs under natural conditions may be restrained by nutrient and light availability.

On the community level, theoretical considerations show how phytoplankton respond to changes in substrate availability by variation of community size structure, even in the absence of grazing (Irwin et al., 2006). In general, small cells have a higher surface-to-volume ratio and can faster satisfy the demand for substrates that are transported towards the cell by diffusion. Accordingly, if we assume that diffusion is a significant process for CO_2-supply to the cell, we principally expect smaller cells to have a selective advantage over larger cells, when CO_2 is limiting. Hence, size spectra of natural phytoplankton communities may be affected by CO_2 diffusive transport processes (up-scaling effects).

To our knowledge, no study has addressed direct effects of CO_2 concentration on the size distribution of cells during phytoplankton blooms so far, or considered selective advantage of cell size variation versus physiological performance with respect to carbon uptake. Here, we investigate the effect of CO_2 availability on the size frequency distribution of particles under conditions mimicking a phytoplankton bloom during a mesocosm experiment.

2 Material and methods

2.1 Set-up of the mesocosm experiment

The study was conducted in the framework of the Pelagic Ecosystem CO_2 Enrichment Study (PeECE II) in spring 2003 at the Large Scale Facility in Bergen, Norway. Nine outdoor mesocosms ($\sim$20 m^3, 9.5 m depth) were filled with unfiltered, nutrient-poor, post-bloom Fjord water, which was pumped from 2 m depth adjacent to the raft and aerated with CO_2/air mixtures in order to achieve 3 different CO_2 levels (190 μatm, 370 μatm and 700 μatm) in triplicates. The general set-up of the mesocosm study has been described in Engel et al. (2005) and Delille et al. (2005) for a similar experiment (PeECE I). Alterations applied during PeECE II are described in Grossart et al. (2006) and are similar to those of PeECE III (Schulz et al., this volume). In order to separate the upper from the lower water column, freshwater was initially added to the surface of each mesocosm, resulting in a halocline at about 5 m depth. During the study, the upper 5 m were continuously mixed using aquarium water pumps. Temperature and salinity profiles were recorded daily using a

CTD. Nutrients were added initially to obtain concentrations in the seawater of 8.6 μmol L^{-1} nitrate, 0.38 μmol L^{-1} phosphate and 12 μmol L^{-1} silicate (Carbonnel and Chou, personal communication). Daily samples were taken from each mesocosm with 4 m long Polyethylene tubes (10 cm diameter), integrating the upper water column and transferred to 20 L carboys. Immediately after sampling the carboys were brought to the lab and subsamples were taken for various analyses. Intrusion of higher salinity water was observed for mesocosm 9 at day 9. Therefore, data from this mesocosm after day 9 were disregarded.

2.2 Carbonate chemistry

Samples for total alkalinity (TA) and total dissolved inorganic carbon (DIC) were poisoned with $HgCl_2$ on collection, stored in bottles with ground glass stoppers and filtered through GF/F filters prior to analysis. TA was measured using the classical Gran potentiometric titration method (Gran, 1952). The reproducibility of measurements was usually within 4 μmol kg^{-1}. Dissolved inorganic carbon (DIC) was measured by coulometric titration (Johnson et al., 1987) with a precision of 2 μmol kg^{-1}. Other CO_2 system variables (pH, CO_3^{2-}, HCO_3^-) were calculated using the CO_2SYS program (Lewis and Wallace, 1998).

The pCO_2 in seawater was measured by means of an equilibrator (Frankignoulle et al., 2001) coupled to an infrared analyzer (Li-Cor 6262). The system was calibrated routinely with air standards with nominal mixing ratios of 0 and 375 μatm of CO_2 (Air Liquide Belgium). Temperature at the inlet of the pump and in the equilibrator was measured simultaneously with two Li-Cor thermosensors. Temperature within the upper mixed 5m ranged between 7.9°C and 10.0°C during the study for all mesocosm. For each measurement of pCO_2, samples for TA were also taken. The pCO_2 was corrected for temperature changes using the dissociation constants of Roy et al. (1993) and TA measurement.

2.3 Particulate organic matter

Total particulate carbon (TPC) and particulate organic nitrogen (PON) were determined by elemental analysis from 1 L (day 0–12) or 0.5 L (day 13–19) samples filtered gently (200 mbar) through precombusted (24 h, 500°C) glass fibre filters (GF/F, Whatman). For determination of POC, filters were fumed for 2 h with saturated HCl to remove all particulate inorganic carbon, and dried for 2 h at 50°C. TPC, POC, and PON were subsequently measured on an Europa Scientific ANCA SL 20–20 mass spectrometer.

2.3.1 Solid particles

Concentration and size distribution of solid particles were determined with a Beckmann Coulter Counter (Coulter Multisizer III), according to Sheldon and Parsons (1978). Three replicate samples of 2000 μL volume were measured daily for each mesocosm using a 100 μm orifice tube. Particles between 2 and 60 μm equivalent spherical diameters (ESD) were binned into 256 size classes. On several days during the bloom, three replicates of 20 ml were counted with a 280 μm orifice to reveal potential abundance of larger particles. These measurements showed that abundance of particles beyond 60 μm ESD was negligible (<1 count/ 10 ml), and the data were therefore not included in this analysis.

2.3.2 Chlorophyll-*a*

Concentration of Chl-*a* was determined fluorometrically from 100 mL samples filtered onto duplicate 0.45 μm cellulose nitrate filters and extracted in 90% acetone overnight. Chl-*a* concentration was measured using a Turner Design fluorometer (model 10-AU) and a standard solution of pure Chl-*a* for calibration.

2.3.3 Flow Cytometry

Phytoplankton counts were performed with a FACSCalibur flow-cytometer (Becton Dickinson) equipped with an air-cooled laser providing 15 mW at 488 nm and with a standard filter set-up. The cells were analysed from fresh prefiltered (30 μm mesh) samples at high flow rate ($\sim$60 μl min^{-1}). Autotrophic groups were discriminated on the basis of their forward light scatter (FLS) and right angle light scatter (RALS) and chlorophyll fluorescence. Counts were assigned to phytoplankton species based on the species signature as obtained from monoclonal cultures and cross-checked by microscopy. Classification of "*Micromonas*-like" cells was adopted from Larsen et al. (1999). Species Listmode files were analysed using WinMDI.

2.4 Statistical treatment of data

Average values are given by the statistical mean ($\bar{x}$) and its standard deviation (SD). Mean values were compared by means of a *t*-test. Significance of the correlation coefficient (r^2) against H_o:ρ=0, was tested by a Student-test according to Sachs (1974):

$$\hat{t} = \frac{r\sqrt{n-2}}{\sqrt{1-r_2}} \quad (1)$$

with n=numbers of observations and the degree of freedom, df=n−2. H_o (r^2=0) is rejected for $\hat{t} \geq \hat{t}_{n-2;\, p}$. The influence of the CO_2-treatment on biological or chemical variables was determined by means of the analysis of variance (ANOVA) or covariance (ANCOVA). The effect of the CO_2-treatment on a linear relationship between two biological or chemical variables was tested by comparing the slopes (b) of the linear regressions (F(x)=b(x)+a), as calculated for each treatment separately, with a *t*-test (Sachs, 1974) with dF=n_1+n_2−4. Significance level of each test was p<0.05.

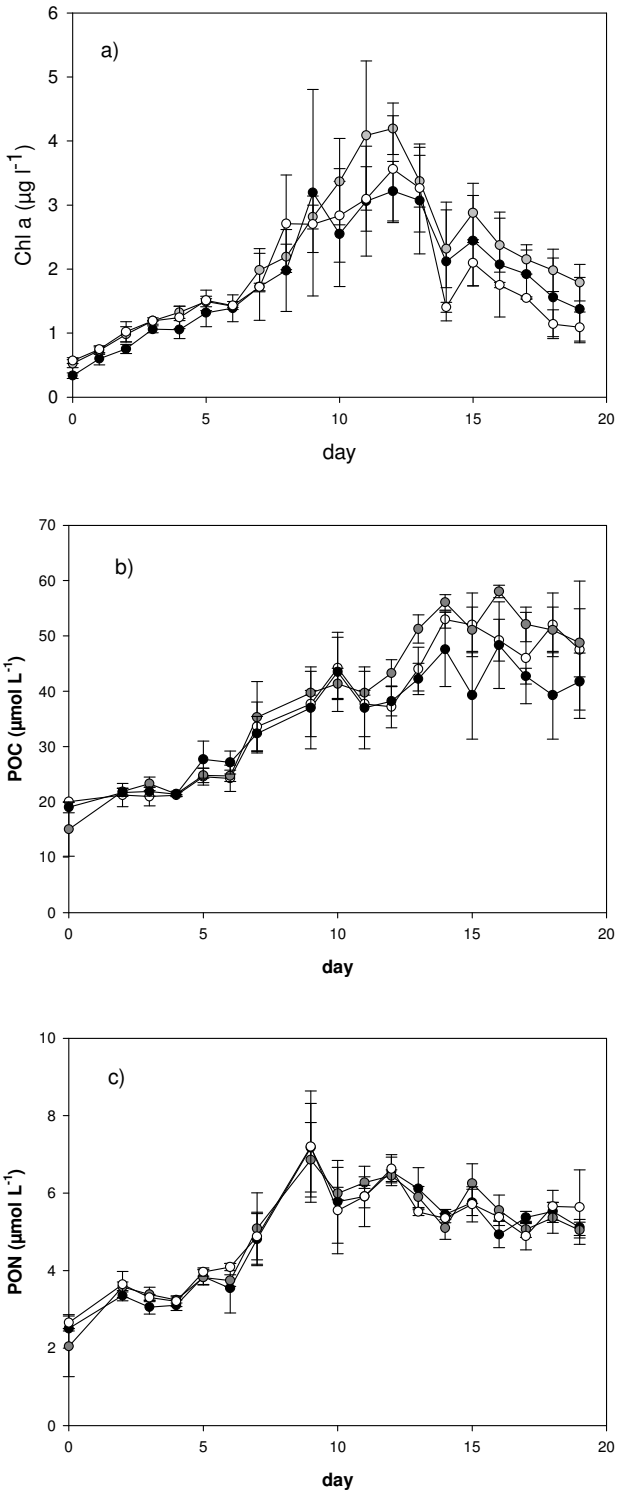

Fig. 1. Temporal development of Chl-*a*, **(a)**, POC, **(b)**, and PON, **(c)**, concentrations as averaged for the three mesocosms in the future, present and past CO_2 treatment, respectively. Error bars denote +/- 1 SD. Open circles: past, grey circles: present, and solid circles: future treatment.

3 Results

3.1 Bloom development

Following the development of the phytoplankton bloom, Chl-*a* increased exponentially in each of the mesocosms until a maximum value was reached between day 9 and day 13 of the experiment (Fig. 1a). The peak of the Chl-*a* concentration coincided with the depletion of nutrients, which was observed for nitrate between day 11 and 12 for all mesocosms (Carbonnel and Chou, personal communication). Thereafter, Chl-*a* concentration declined until the end of the experiment. The bloom can be divided into a pre-bloom phase that covered the first week of the experiment, a bloom phase during the second week, and a post-bloom phase towards the end of the experiment. Inevitable variations during the initialisation procedure introduced small variability among all mesocosms. Therefore, we find deviations regarding the timing of the maximum Chl-*a* concentration and the onset of decline phase within the CO_2 treatments (one to three days). For later reference we defined more narrow windows for the three phases of the experiment that can clearly be differentiated in all mesocosms; the pre-bloom: days 1–3, the bloom peak: Chl-*a* max $\pm$1 day, and the post bloom: days 18–20.

With respect to the CO_2-treatment no significant difference in Chl-*a* concentration or in the timing of the maximum concentration were observed. Nutrient draw-down was not significantly different among the CO_2 treatments at any time of the experiments (Carbonnel and Chou, personal communication) either.

Particulate organic carbon (POC) concentration started with $17\pm3.5\,\mu$mol L^{-1} and increased throughout the study in all mesocosms to final values of 42–49 μmol L^{-1} (Fig. 1b). POC concentration was not related to CO_2 concentration (ANOVA). Particulate organic nitrogen (PON) concentration was initially $2.4\pm0.5\,\mu$mol L^{-1} and increased to maximum values of $7.1\pm1\,\mu$mol L^{-1} on day 9 of the bloom (Fig. 1c). PON concentration was remarkably similar in all mesocosms and no significant effects of the CO_2 treatment on PON concentration was determined (ANOVA).

Maximum molar [POC]:[PON] ratios were observed during the post-bloom phase with 8.6 ± 0.8, 10 ± 1.0 and 9.7 ± 1.3 for the past, present and future CO_2 treatment, respectively. No significant CO_2 effect on the carbon-to-nitrogen (C:N) ratios of POM was determined (ANOVA).

3.2 Particle abundance and size distribution

More than 95% of all particles between 2 and 60 μm equivalent spherical diameter (ESD) were detected with the Coulter Counter in the size range between 2 and 10 μm ESD. Larger particles were counted randomly, with abundances that fall into the range of uncertainty (variability) of one treatment, represented by three mesocosms (replicates). Total abundance of Coulter Counter particles (CCP) measured

shortly after initialisation in all mesocosms, was indifferent among treatments, yielding an average of 7750 ±560 counts mL^{-1}. The CCP abundance increased exponentially during the bloom until maximum concentrations were reached between day 11 and day 15 (day 9 for M9) (Fig. 2). Maximum CCP abundances, as averaged separately for the three CO_2 treatments, were 43 000±5000 counts mL^{-1} for the past, and 52 600±9500, and 42 500±11600 counts $mL^{-1}$for the present and future CO_2 treatment, respectively. The net specific growth rate (μ_t) for CCP during the phase of exponential growth was calculated for each mesocosm: μ_t= [ln(C_i)-ln(C_{i-1})]/[t_i-t_{i-1}], with ln(C_i) and ln(C_{i-1}) being the natural logarithm of CCP concentrations at two consecutive days. Maximum values for μ_t ranged between 0.30 d^{-1} (M1) and 0.68 d^{-1} (M7). No significant effects of the CO_2 treatment on the parameter (μ_t) or on the maximum values for μ_t were identified.

The size frequency distributions, or size spectra, of CCP, changed over time in all mesocosms (Fig. 3). Size spectra were not significantly different for the three treatments during the pre-bloom phase (ANOVA), but developed differently during growth of the phytoplankton community. Given the present day CO_2 treatment as a reference, we find two distinct maxima in the size spectra, one around 2 μm ESD and another close to 5 μm ESD. Compared to the present day CO_2 treatment, there was a lack of the larger population in the past CO_2 treatment, whereas a drastic reduction of particles abundance was observed at small size (<4 μm) in the future CO_2 treatment (Fig. 3). These distinct differences persisted during the post-bloom phase, but with an increase in variability within the individual treatments.

Differences in size distribution were reflected in significant differences of the median particle size of CCP among the CO_2 treatments over the course of the experiment (ANOVA, $p<0.001$, t-test$_{\text{future-present}}$ $p<0.005$, t-test$_{\text{present-past}}$ $p<0.001$; Fig. 4). The highest value for median particle size of CCP was observed on day 7 in the future CO_2 treatment with 4.23±0.11 μm ESD (mean ±1 SD calculated from three mesocosms). The maximum value for median size in the present day CO_2 treatment was observed at day 7 also, but with a slightly smaller value of 4.12±0.10 μm ESD. Clearly smaller particles were observed in the mesocosms of the past CO_2treatment, yielding a maximum median size of 3.70±0.05μm ESD at day 5. The temporal development of the median size of particles followed similar dynamics irrespectively of the CO_2 concentration; i.e. the median size increased at the beginning of the experiment, had a maximum value during mid or late pre-bloom, a declining phase during the peak of the bloom, and varied only little during the post-bloom phase.

However, median sizes in past CO_2 treatment deviated from the present day or future CO_2 already on day 4. Moreover, the maximum value of median sizes was observed on day 5 in past CO_2 treatment and thus two days earlier than in the other two treatments. This indicates that the absolute

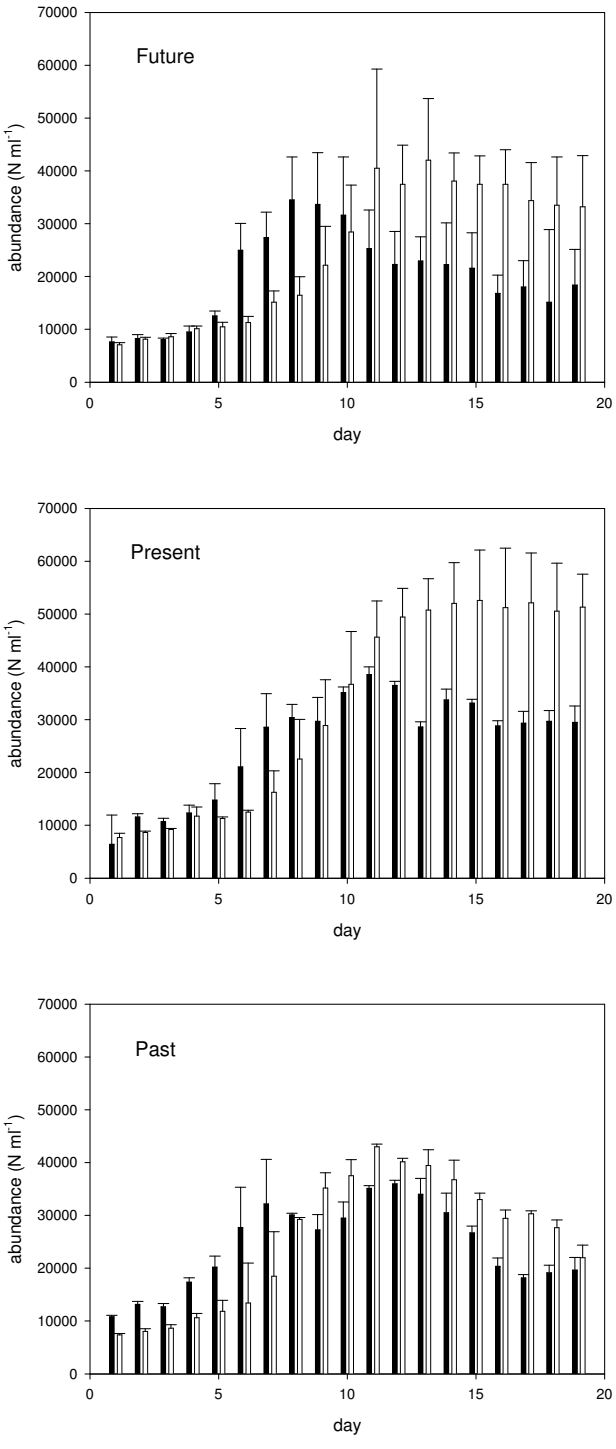

Fig. 2. Temporal changes in the average total abundance of autotrophic cells (solid bars) and total particles (open bars) as determined by Flow Cytometry and Coulter Counter, respectively, averaged for the future, present and past CO_2 treatment, respectively. Error bars denote +/- 1 SD.

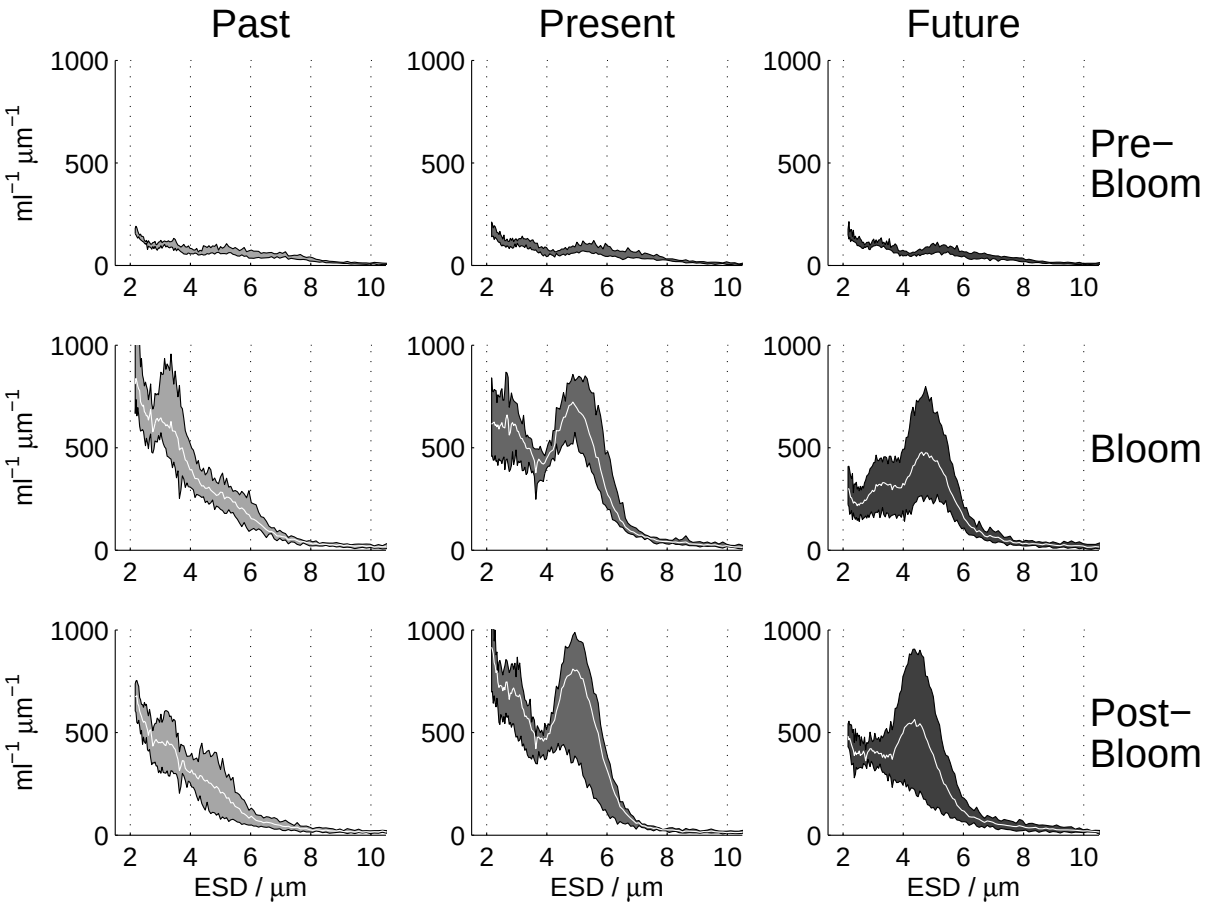

Fig. 3.
Spectral distribution of Coulter Counter particles in the size range 2-10 μm ESD during the pre-bloom, bloom and post-bloom phases of the experiments for the three different CO_2 treatments. Figures show spectral distributions of particles (counts ml^{-1} μm^{-1}) for the three mesocosms of each treatment during days 1-3 in the pre-bloom, and days 18–20 in the post-bloom phase. For the bloom phase, the time span includes the day of Chl-*a* maximum for each mesocosm and $\pm$1 day. The shaded areas enclose all realisations of the respective days; white solid lines show mean trajectories.

value of median size as well as the timing of the saddle point was affected by the CO_2-treatment.

Effects of the CO_2 treatment on particles size were also reflected in the ratio of the total surface to total volume (TS:TV), calculated as

$$\mathrm{TS:TV} = \sum_i^{ii} \left\{ \pi (\mathrm{ESD}_i)^2 \times n_i \right\} / \sum_i^{ii} \left\{ 1/6\pi (\mathrm{ESD}_i)^3 \times n_i \right\} \quad (2)$$

with ESD_i being the smallest (2 μm) and ESD_{ii} the largest (60 μm) size class observed.

During the 7-day period of the bloom of the phytoplankton community, TS:TV ratios were significantly related to DIC concentration of seawater ($p<0.001$) and decreased with increasing DIC (Fig. 5).

3.3 Phytoplankton community composition

Total number (N) of autotrophic cells, as determined by Flow Cytometry in the size range 1.5–30 μm, was 6300$\pm$1700 N mL^{-1} initially and increased throughout the experiment in all mesocosms (Fig. 3a–c). Maximum average phytoplankton abundance was 36000$\pm$1500 N mL^{-1}, 38500$\pm$9450 N mL^{-1} and 34500$\pm$3930 N mL^{-1} for the past, present day and future CO_2 treatment, respectively. During the course of the experiment, total abundance of phytoplankton cells differed significantly among the treatments (ANOVA, $p<0.005$), with the future CO_2 treatment having the lowest autotrophic cell abundance (t-test, $p<0.001$). Comparing the total abundance of phytoplankton (within size range 1.5–30 μm) with total CCP abundance in the size range 2–60 μm ESD revealed a similar temporal development (Fig. 3a–c). However, the Flow Cytometry data showed systematically higher total phytoplankton abundance during the pre-bloom and bloom

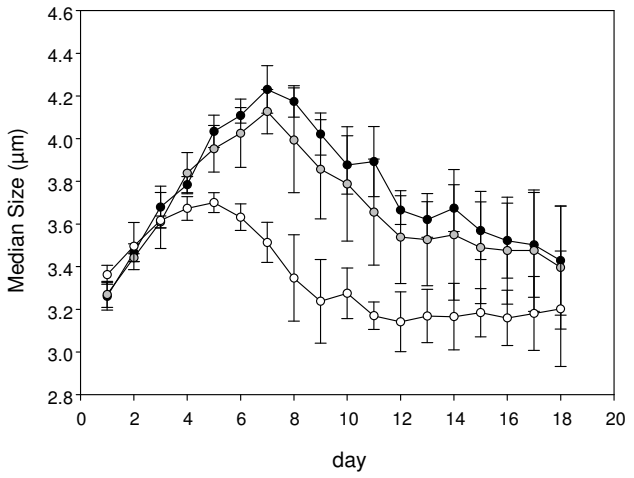

Fig. 4. Median size of Coulter Counter particles in the size range 2–60 μm ESD, averaged for three mesocosms per CO_2 treatment over the course of the experiment. Open circles: past, grey circles: present, and solid circles: future treatment. Error bars denote +/- 1 SD.

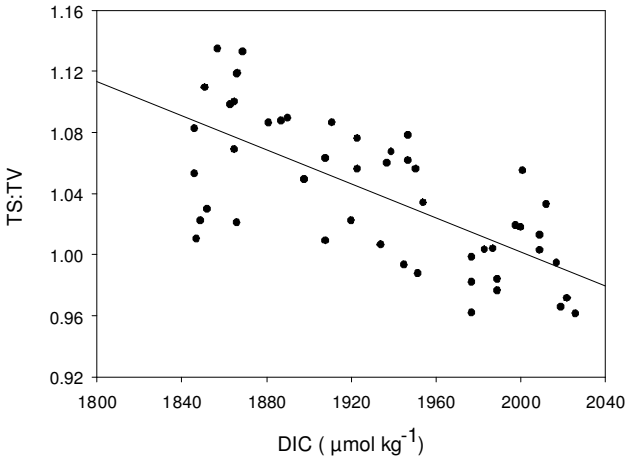

Fig. 5. The total surface (TS) to total volume (TV) ratio of particles determined with the Coulter Counter in the size range 2–60 μm ESD was significantly related to the concentration of DIC in the seawater ($p<0.001$). Data: bloom phase of each mesocosm; n=50.

phase up to day 10 of the experiment. This can be attributed to the lower size detection limit of the Flow Cytometer. After day 10, the number of CCP increased over the number of phytoplankton, indicating the transition from a small-celled autotrophic community to a mixed community, including heterotrophic organisms and detritus particles. In general, the relative contribution of autotrophic cells to total particles was highest in the past CO_2 treatment and similar in the present day and the future CO_2 treatment.

The species composition of phytoplankton, as determined by Flow Cytometry, indicate that the phytoplankton community was initially similar in all enclosures and was dominated, in terms of numbers, by cells with a signature similar that of the phytoflagellate *Micromonas spp.*; termed *Micromonas*-like in the following (Fig. 6). Other major phytoplankton species included diatoms, specifically *Nitzschia spp.*, the coccolithophore *Emiliania huxleyi*, and the nanoflagellate *Phaeocystis spp.*. During the bloom, the relative abundance of phytoplankton species developed significantly differently in the CO_2 treatments (ANOVA, $p<0.05$). In the past CO_2 treatment, populations of small (<4 μm) unidentified autotrophic cells grew rapidly and dominated the community structure during the bloom to a large extend. The *E. huxleyi* population was most prominent in the present, and, although to a smaller degree, in the future CO_2 treatment. The *E. huxleyi* population was determined by the Coulter Counter in the size range 4–8 μm ESD and identified in the future and present day mesocosms by clear peaks. Because no significant differences between the future and present day CO_2 treatment were observed for the median particle size in this 4–8 μm ESD size window, we can assume that the size of the *E. huxleyi* population itself did not vary significantly with CO_2. Diatoms (>4 μm) contributed between 4 to 12% to total phytoplankton abundance with the higher values observed during the pre-bloom phase. Within the group of diatoms, a smaller size population of *Nitzschia* was differentiated from a group of larger (>8 μm) diatoms. For both diatom groups, no significant differences in terms of absolute and relative abundance among the CO_2 treatments were observed (ANOVA, $p>0.05$). During the post-bloom phase the average phytoplankton composition of the future and present CO_2 treatment approached those observed for the past treatment during the bloom and no significant CO_2 related differences were determined.

4 Discussion

The aim of this study was to test the hypothesis that CO_2 concentration can affect the size distribution of cells during the course of a phytoplankton bloom. Our results revealed that the size distribution of suspended particles in the range 2–60 μm ESD differed significantly among the three CO_2 treatments during the bloom phase itself, when biological processes were dominated by autotrophic growth. There were several indications for particles tending to be smaller at lower CO_2 concentration and larger at higher CO_2 concentration relative to the present day concentration, expressed by the median size of suspended particles, by the total-surface-to-total-volume ratio, and by the multi-modal distribution of particle size. Changes in CO_2 also led to significant structural effects on the autotrophic community, as indicated by the different abundance of phytoplankton taxa using Flow Cytometry. Thereby, the major phytoplankton populations were affected differently. While some populations such as diatoms seemed to be insensitive to the CO_2 treatment, others

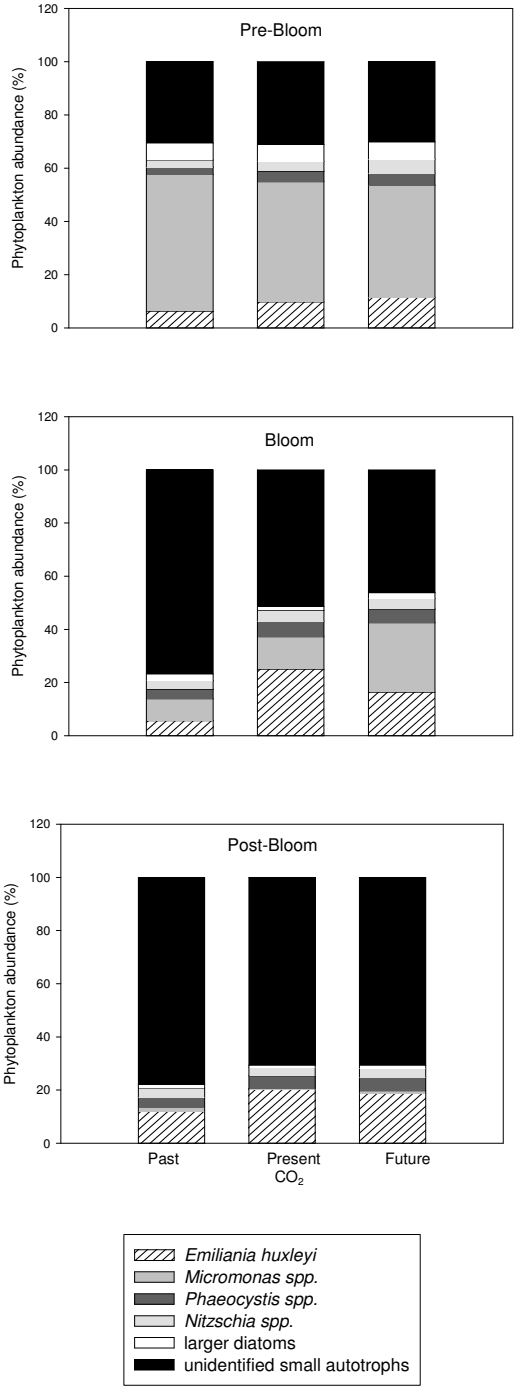

Fig. 6. Relative composition of the phytoplankton community in the size range 1.5–30 μm during the different phases of the experiment and separated for the three CO_2 treatments. Data are averages of three mesocosms per treatment calculated for days 1–3 in the pre-bloom, and days 18-20 in the post-bloom phase. For the bloom phase, averages were calculated from the data of the day of Chl-*a* maximum for each mesocosm and $\pm$1 day.

increased in abundance with CO_2, or were most abundant at present day CO_2.

4.1 CO_2 effects on size distribution of suspended particles

Causes for changes in the size distribution of autotrophic cells can be manifold. In general, metabolic processes, such as growth, nutrient and light acquisition, or respiration, are related to organism size (Peters, 1983). Grazers often select their prey according to size, and the settling rate of most types of marine particles increases with size. For marine phytoplankton, metabolic scaling has previously been shown for some processes such as nutrient uptake, photosynthesis and growth (Finkel et al., 2004). For others, such as respiration, the existence of size dependence has been questioned (Falkowski and Owens, 1978). Moreover, the relative surface area can be of greater importance than cell diameter, mass or volume with respect to processes such as nutrient uptake, because it is the surface that interferes with the outer medium containing the substrate reservoir. The relative surface area of a phytoplankton cell increases with decreasing size, but also with increasing eccentricity of the cells. Small or elongated phytoplankton species should be better competitors for resources, in particular when these limit biomass production (Grover, 1989). Therefore, small-sized phytoplankton cells are likely to dominate under oligotrophic conditions, whereas elevated nutrient concentration induce growth of larger cells (Irwin et al., 2006).

During this study, significant effects of the CO_2 treatment on particle size distribution were most obvious during the time of the bloom when autotrophic cells dominated particle abundance. This indicates a bottom-up effect of CO_2 on size on the phytoplankton community level. Particle size during this study, however, was derived from volume and expressed as equivalent spherical size without any additional information on the shape of the cells. Information gained from the Flow-Cytometer and from microscopy nevertheless revealed that most species in the size range 1.5–30 μm were indeed rather spherical, with the exception of *Nitzschia* spp.. Although the distal length of *Nitzschia spp.*. is relatively large, their proximal size is small and thus the volume is small. However, abundance of *Nitzschia spp.* was not significantly different among the CO_2 treatments. Hence, eccentricity of cells did not bias the observation of a general increase in cell size with increasing CO_2 during this study.

During the bloom phase, the observed differences in particle size spectra and median particle size were related to differences in phytoplankton community composition. *Micromonas*-like cells and *E. huxleyi*, for example were more abundant in the present day and future than in the past CO_2 treatment. In the latter, smaller autotrophic nanoplankton clearly dominated the bloom by number. Size variations within individual species were presumably not related to the CO_2-treatment. However, at least for *E. huxleyi* potential changes in the protoplast size may have been masked by

simultaneous changes in coccosphere size due to potential effect of CO_2 on calcification (Riebesell et al., 2000). During a similar mesocosm study (PeECE I), when the phytoplankton community was clearly dominated by *E. huxleyi*, Engel et al. (2005) observed that the sizes and weights of coccospheres were largest at low CO_2. During PeECE I, no significant differences in the phytoplankton community were observed with respect to the CO_2 treatment. One reason for the different outcome of PeECE I and II with respect to CO_2 influence on phytoplankton community composition may be that nutrients in the PeECE I-experiment were added in a NO_3:PO_4 ratio of 30 and without any additional supply of silicate in order to favour the blooming of *E. huxleyi*. In the present study N:P:Si were added in "Redfield-ratio" in order to allow for a mixed assemblage of diatoms, coccolithophores and other autotrophic species.

4.2 CO_2 effects on phytoplankton community composition

Recent investigations on CO_2 acquisition in marine phytoplankton species demonstrated that many phytoplankton groups including diatom species such as *Skeletonema costatum* efficiently apply carbon concentrating mechanisms (CCMs) (Rost et al., 2003). CCMs can be understood as a physiological regulation of CO_2 acquisition to maintain high photosynthetic rates even at reduced CO_2 concentration. Goldman (1999) observed no reduction in cell growth of large diatom species until CO_2 concentrations fell as low as 4 μmol L^{-1}, indicating that growth of these species was not depending on the diffusional supply of CO_2, but was supported by CCMs. During this study the abundance of diatoms was not significantly different among the CO_2 treatments, supporting the idea that diatoms do not suffer from changes in CO_2 concentrations over a relatively wide range. Abundance of *E. huxleyi*, in contrast, was significantly reduced in the past CO_2 treatment. This is in accordance with our expectations, since *E. huxleyi* has been shown to have a low affinity to CO_2 (Rost et al., 2003). Abundance of *Micromonas*-like cells increased with increasing CO_2, indicating that this species does not apply CCMs efficiently, either. However, the strongest response to CO_2 concentration was observed in the group of small autotrophs that grew abundantly in the past CO_2 treatment, but little in the future CO_2 treatment. Changes in the abundance of these small cells were mainly responsible for the changes in size spectra compared to the present day treatment.

Interestingly, it was the group of small-celled algae that numerically dominated phytoplankton community at low CO_2, and not larger diatoms, which we expected to be good competitors based on their high CO_2 affinity and physiological capability. Microscopic observations revealed that the group of small cells comprised various phytoplankton taxa (Martin-Jezquel, personal communication), indicating that size itself was selected in the low CO_2 treatment. Because we did not determine CCM operations in phytoplankton during this study, we can only speculate about possible explanations for the observed CO_2-effects on phytoplankton abundance and size distribution. First, CCMs in diatoms, or other species, may have been co-limited by phosphate or light availability (Young and Beardall, 2005, Beardall et al., 2005) and were not efficient enough to give a competitive advantage at low CO_2 concentration. Phosphate concentrations during this study decreased strongly within the first week, while at the same time NO_x:PO_4^{3-} ratios increased up to 28 (Carbonnel and Chou, personal communication), indicating high phosphorus demand of phyto- and bacterioplankton cells. To prevent depletion, PO_4^{3-} was added again to all mesocosms on day 8. By this time differences in the particle size spectra had already evolved (Fig. 4). Thus, we cannot exclude that P limitation may have affected CCMs of algal species and was co-limiting active C- uptake in the past CO_2 mesocosms. If P were the potentially limiting nutritious element, we would expect that species allocating PO_4^{3-} efficiently for reproduction have an advantage over those species, which additionally need to allocate PO_4^{3-} for CCM operation. Under these circumstances, reduction of cell size would be beneficial to circumvent both P- and CO_2 limitation and may help to explain the observed relationship between size and DIC availability during this study. We may then speculate that future effects of elevated CO_2 concentration on the size spectrum of phytoplankton communities may especially occur in oceanic regions, where P is limiting phytoplankton production.

Another hypothesis would be that CCMs only acted as a surplus to carbon acquisition and were expressed equally well in all phytoplankton species observed in the past CO_2 treatment. Cassar et al. (2004) estimated that 50% of carbon uptake in a natural diatom population was comprised by HCO_3^- uptake, the remaining 50% by CO_2. Reduction of cell size may therefore be pivotal to enhance the fraction of CO_2 taken up by diffusion, and to accelerate growth rates of small cells. Certainly, more investigations are needed to elucidate the interplay between size and physiological regulation of carbon uptake during natural phytoplankton blooms, and the impact on carbon acquisition and species selection in the future ocean.

During the post-bloom phase, species composition was quite similar in all CO_2 treatments, indicating that factors other than CO_2 were influencing species distribution at this time.

4.3 Potential consequences for carbon cycling

Particle size distribution and phytoplankton species composition were rather similar in the present day and future CO_2 treatment, and clearly different from the past CO_2 treatment. This is in accordance with the non-linear relationship between CO_2 concentration and primary production, indicating that the selective pressure towards a larger relative surface area, i.e. cell size reduction, for species relying on CO_2

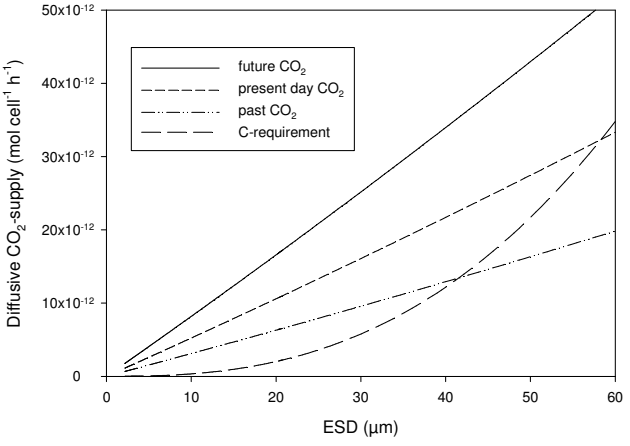

Fig. 7. Theoretical rates for the diffusive CO_2-supply to the cell during the peak of the bloom for the different CO_2 treatments as a function of cells size. The dashed line indicates the theoretical carbon requirement for maintaining maximum cell quota at a growth rate of 1 day^{-1}. Further information is given in the text.

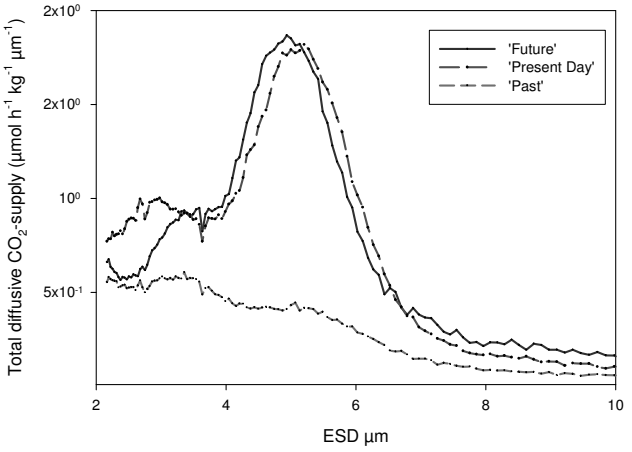

Fig. 8. Spectral distribution (2–10 μm ESD) of total diffusive CO_2 supply calculated for the peak of the bloom in the three different CO_2 treatments.

uptake, whatsoever, increase with decreasing CO_2 concentration. As mentioned above, we do not have information about potential enhancement of carbon uptake due to CCM operations in phytoplankton during this study. In order to estimate potential differences in carbon acquisition within the three CO_2 treatments due to the observed differences in cell size, we can only estimate the treatment effect on the diffusive supply with CO_2. To estimate the spectral distribution of CO_2 supply during the bloom phase in the three CO_2 treatments, we calculated theoretical rates of CO_2 supply to the cell according to the simplified model of Riebesell et al. (1993) (Fig. 7); see also Gavis and Ferguson (1975) and Wolf-Gladrow and Riebesell (1997) for further information. In alteration to Riebesell et al. (1993) CO_2-supply rates were calculated for each of the 256 size classes ranging from 2 μm ESD to 60 μm ESD using the average observed CO_2 concentrations during the 'bloom-period', i.e. 22.34, 14.28 and 8.49 μmol kg^{-1} for the future, present day and past CO_2 treatment, respectively. A conversion factor (ak) of 400 was assumed, accounting for the HCO_3^-–CO_2 equilibrium at the observed pH- and temperature range. The half-saturation constant (Km) was fixed to 10 μmol kg^{-1}, assuming that this is a representative value for a mixed phytoplankton community of diatoms, coccolithophores and *Phaeocystis spp.* However, varying Km from 0.5 to 20 had only little effect on the estimates for CO_2 fluxes (<0.1%) in our model. To calculate the maximum CO_2–supply rate ($V_{max}=\mu_{max}\times Q_c$) for each size class, the maximum growth rate of cells (μ_{max}, d^{-1}) was calculated with a parameterization that scales with cell volume (V, μm^3):$\mu_{max}=a(V)^b$; with a=5.37, b=–0.25 after Irwin et al. (2006); the carbon cell quota (Q_c; pg C) was calculated using $Q_c=d(V)^e$, with d=0.436, e=0.863 after Verity et al. (1993). The results of these calculations show that the spectral distributions of total diffusive CO_2-supply during the time of the bloom were different in the three CO_2 treatments (Fig. 8). With the exception of the very low size range (<4 μm ESD), the estimated total CO_2-supply was higher at all size classes in the present day and future CO_2 treatment than in the past. Only at particle sizes <4 μm ESD, the higher abundance of particles in the past CO_2 treatment could partially compensate for the lower supply rates per cell. Integration over the size range 2–60 μm ESD yielded similar values for potential CO_2-supply for the future and present day CO_2 treatment with 100 μmol h^{-1} kg^{-1} and a much lower value for the past CO_2 treatment with 46 μmol h^{-1} kg^{-1}. It has to be emphasized that these rates address only the aspect of diffusive flux of CO_2 to the cells. Averaged rates of primary production during this experiment yielded much lower values (Egge et al., 2007). Nevertheless, our calculations indicate that the total supply of cells with CO_2 was lowest in the past treatment despite the strong increase in the abundance of small cells, whereas the present day and future CO_2 treatment may have been equally productive despite the lower abundance of particles and autotrophic cells in the latter. A potentially higher CO_2-supply of cells in the future and present day CO_2 treatment is in accordance with earlier observations obtained during PeECE I, showing that the ΔDIC:Δ cell ratio increased with CO_2 concentration (Engel et al., 2005).

It is interesting to note that neither the potential differences in CO_2 supply nor the structural differences in the size spectra and in the phytoplankton community composition were reflected in the standing stocks of POC and PON. One might argue that PON production was rather related to the supply of inorganic nitrogen than to the availability of carbon, as inorganic nitrogen became exhausted in all mesocosms during the bloom development. As a consequence of the relative higher abundance of smaller particles, total particle volume

was lower in the past CO_2 treatment. The observation that PON concentration in the past treatment was not significantly different from those in the present-day and future treatment allows for two interpretations: either smaller particles contributed to PON in a higher proportion, or other particulate material that was not detected with the Coulter Counter, out of the size range 2–60 μm ESD, such as bacteria, contributed to PON to a higher degree. In fact, Verity et al. (1993) showed that the scaling exponent for the increase of nitrogen and carbon with cell volume is less than 1, and thus the volume of cells increases faster with size than the concentration of elemental components. Moreover, the scaling exponent for nitrogen is lower than for carbon leading to an increase of C:N ratios with cell size. However, estimates for the carbon and nitrogen content of cells vary even for cultures of the same species (Montagnes et al., 1994) and may not be representative for particles encountered during this study.

4.4 Potential consequence for ecosystem functioning

Structural changes in the size distribution of particles were observed during this mesocom experiment, together with changes in the composition of the phytoplankton community. This response to changes in CO_2 cannot be explained with a unique scaling law (Enquist et al., 1998; Belgrano and Brown, 2002). Rather the differences observed are expected to include responses to micro-zooplankton grazing as well. Therefore, our results suggest a complex, yet unresolved, interplay of various size-dependent effects due to CO_2 supply, nutrient uptake and grazing. In general, pico- and small nanoplankton cells with a large surface-to-volume ratio are efficient in taking up resources, of which only a small fraction is needed for enzymes involved in C-fixation. These cells have a potential advantage under low substrate, and low CO_2 conditions but are susceptible to grazing by small protozoans and other micro-zooplankton. Larger phytoplankton cells have a smaller surface-to-volume ratio and are less competitive in terms of resource uptake, but they can allocate more luxury resources that may allow them to better compensate environmental changes (e.g. better acclimation to varying environmental factors such as CO_2). Their larger size can moreover be advantageous to escape micro-zooplankton grazing. Intermediate-sized cells have to find a balance between resources needed purely for growth, those that enhance physiological acclimation, and those resources that support predation defence. Thus, intermediate-sized nanophytoplankton have no obvious advantage when it comes to escape grazing pressure, but also with respect to resource uptake. Instead, they rely on a fine balance (trade-off).

Exceptions may be given for species growing in chains, colonies or filaments, such as *Phaeocystis* and diazotrophic cyanobacteria.

Overall, CO_2 induced changes in carbon utilization within the phytoplankton community are likely transferred to higher trophic levels, but may also change the quality of DOM. During this experiment, CO_2-sensitivity was found within a size spectrum that is rather narrow compared to the total phytoplankton size range (i.e. $1–5\times10^3$ μm) that can be observed in the ocean. The sensitive size range overlaps with those inherent to the microbial food web of pico- and nanoplankton. The microbial food web comprises a tight linkage between trophic interactions and DOM utilisation (Azam et al., 1983). Therefore, CO_2 related changes in the size distribution of phytoplankton involved in the microbial food web must be expected to affect DOM quality in conjunction with a response in micro-zooplankton grazing.

Acknowledgements. The staff at the Marine Biological Station, University of Bergen, in particular T. Sørlie and A. Aadnesen, and the Bergen Marine Research infrastructure (RI) are gratefully acknowledged for support in mesocosm logistics. We also thank A. Terbrüggen for technical assistance. V. Carbonnel and L. Chou are gratefully acknowledged for providing information on nutrients. This study was supported by EU-TMR contract no HPRI-CT-2002-00181 and by the Helmholtz Association contract no HZ-NG-102.

Edited by: J. Middelburg

References

Azam, F., Fenchel, T., Field, J. G., Gray, J. S., Meyer-Reil, L. A., and Thingstad, F.: The ecological role of water-column microbes in the sea, Marine Ecology-Progress Series, 10, 257–263, 1983.

Badger, M. R., Andrews, T. J., Whitney, S. M., Ludwig, M., Yellowlees, C. D., Leggat, W., and Price, G. D.: The diversity and coevolution of Rubisco, plastids, pyrenoids, and chloroplast-based CO_2-concentrating mechanisms in algae, Canadian Journal Botany, 76, 1052–1071, 1998.

Barcelos e Ramos, J., Biswas, H., Schulz, K. G., LaRoche, J., and Riebesell, U.: Effect of rising atmospheric carbon dioxide on the marine nitrogen fixer *Trichodesmium*, Global Biogeochem. Cy., 21, GBC2028, doi:10.1029/2006GB002898, 2007.

Belgrano, A. and Brown, J. H.: Oceans under the macroscope, Nature, 419, 128–129, 2002.

Beardall, J., Roberts, S., and Raven, J. A.: Regulation of inorganic carbon acquisition by phosphorus limitation in the green alga *Chlorella emersonii*, Canadian Journal of Botany, 83, 859–864, 2005.

Boyd, P. W. and Doney, S. C.: Modelling regional responses by marine pelagic ecosystems to global change, Geophys. Res. Lett., 29(16), 1806, doi:10.1029/2001GL014130, 2002.

Caldeira, K. and Wickett, M. E.: Anthropogenic carbon and ocean pH, Nature, 425, 365, 2003.

Cassar, N., Laws, E. A., and Bidigare, R. R.: Bicarbonate uptake by Southern Ocean phytoplankton, Global Biogeochem. Cy., 18, GB2003, doi:101029/2003GB002166, 2004.

Chen C. Y. and Durbin, E. G.: Effects of pH on the growth and carbon uptake of marine phytoplankton, Marine Ecology Progress Series, 109, 83–94, 1994.

Delille B., Harlay, J., Zondervan, I., Jacquet, S., Chou, L., Wollast, R., Bellerby, R. G. J., Frankignoulle, M., Borges, A. V.,

Riebesell, U. and Gattuso, J.-P.: Response of primary production and calcification to changes of pCO_2 during experimental blooms of the coccolithophorid *Emiliania huxleyi*, Global Biogeochem. Cy., 19, GB2023, doi:10.1029/2004GB002318, 2005.

Egge, J. K., Thingstad, T. F., Engel, A., and Riebesell, U.: Primary production during nutrient-induced blooms at elevated CO_2 concentrations, Biogeosciences Discuss., 4, 4385–44410, 2007, http://www.biogeosciences-discuss.net/4/4385/2007/.

Engel, A., Delille, B., Jacquet, S., Riebesell, U., Rochelle-Newall, E., Terbrüggen, A., and Zondervan, I.: TEP and DOC production by *Emiliania huxleyi* exposed to different CO_2 concentrations: A mesocosm experiment, Aquatic Microbial Ecology, 34, 93–104, 2004.

Engel, A., Zondervan, I., Aerts, K., Beaufort, l., Benthien, A., Chou, L., Delille, B., Gattuso, J. P., Harlay, J., Heemann, C., Hoffmann, L., Jacquet, S., Nejstgaard, J., Pizay, M. D., Rochelle-Newall, E., Schneider, U., Terbrueggen, A., and Riebesell, U.: Testing the direct effect of CO_2 concentration on a bloom of the coccolithophorid *Emiliania huxleyi* in mesocosm experiments, Limnol. Oceanogr., 50, 493–507, 2005.

Enquist, B. J., Brown, J. H., and West, G. B.: Allometric scaling of plant energetics and population density. Nature, 395, 163–165, 1998.

Falkowski, P. and Owens, T. G.: Light-shade adaptation, Plant Physiology, 66, 592–595, 1978.

Finkel, Z. V., Irwin, A. J., and Schofield, O.: Resource limitation alters the 3/4 size scaling of metabolic rates in phytoplankton, Marine Ecology Progress Series, 273, 269–279, 2004.

Frankignoulle, M., Borges, A. V., and Biondo, R.: A new design of equilibrator to monitor carbon dioxide in highly dynamic and turbid environments, Water Res., 35, 1344–1347, 2001.

Gao K., Aruga Y., Asada K., and Kiyohara, M.: Influence of enhanced CO_2 on growth and photosynthesis of the red algae *Gracilaria sp.* and *G. chilensis*, J. Appl. Phycol., 5, 563–571, 1993.

Gavis, J. and Ferguson, J. F.: Kinetics of carbon dioxide uptake by phytoplankton at high pH, Limnol. Oceanogr., 20, 211–221, 1975.

Goldman J. C.: Inorganic carbon availability and the growth of large marine diatoms, Marine Ecology Progress Series, 180, 81–91, 1999.

Gran, G.: Determination of the equivalence point in potentiometric titrations of seawater with hydrochloric acid, Oceanology Acta, 5, 209–218, 1952.

Giordano, M., Beardall, J., and Raven, J. A.: Co_2 concentrating mechanisms in algae: mechanisms, environmental modulation, and evolution, Annual Plant Biology, 56, 99–131, 2005.

Goerike, R. and Fry, B.: Variations of marine plankton $\delta^{13}C$ with latitude, temperature, and dissolved CO_2 in the world ocean, Global Biogeochem. Cy., 8, 85–90, 1994.

Grover, J. P.: Influence of cell shape and size on algal competitive ability, J. Phycol., 25, 402–405, 1998.

Irwin, A. J., Finkel, Z. V., Schofield, O. M. E., and Falkowski, P. G.: Scaling-up from nutrient physiology to the size-structure of phytoplankton communities, Journal of Plankton Research, 28, 459-471, 2006.

Grossart, H.-P., Allgaier, M., Passow, U., and Riebesell, U.: Testing the effect of CO_2 concentration on the dynamics of marine heterotrophic bacterioplankton, Limnol. Oceanogr., 51, 1–11, 2006a.

Hinga, K. R.: Effects of pH on coastal marine phytoplankton, Marine Ecology Progress Series, 238, 281–300, 2002.

Houghton J. T., Ding, Y., Griggs, D. J., Noguer, M., Van der Linden, P. J., Dai, X., Maskell, K., and Johnson, C. A.: Climate Change 2001: The Scientific Basis: Contribution of Working Group I to the Third Assessment Report of the Intergovernmental Panel of Climate Change, Cambridge University Press, 2001.

Hutchins, D. A., Fu, F.-X., Zhang, Y., Wagner, M. E., Feng, Y., Portune, K., Bernhardt, P. W., and Mulholland M. R.: CO_2 control of *Trichodesmium* N_2 fixation, photosynthesis, growth rates, and elemental ratios: Implications for past, present and future ocean biogeochemistry, Limnol. Oceanogr., 52, 1293–1304, 2007.

Irwin, A. J., Finkel, Z. V., Schofield, O. M. E., and Falkowski, P. G.: Scaling-up from nutrient physiology to the size-structure of phytoplankton communities, J. Plankton Res., 28, 459–471, 2006.

Johnson, K. M., Williams, P. J., Brandstrom, L., and Sieburth, J.: Coulometric total carbon analysis for marine studies: automation and calibration, Marine Chemistry, 21, 117–133, 1987.

Larsen, A., Castberg, T., Sandaa, R. A., Bussaard, C. P. D., Egge, J., Heldal, M., Paulino, A., Thyrhaug, R, van Hannen, E. J., and Bratbak, G.: Population dynamics and diversity of phytoplankton, bacteria and viruses in a seawater enclosure, Marine Ecology Progress Series 221, 47–57, 2001.

Lewis, E. and Wallace, D. W. R.: Program Developed for CO_2 System Calculations. ORNL/CDIAC-105, Carbon Dioxide Information Analysis Center, Oak Ridge National Laboratory, US Department of Energy, Oak Ridge, Tennessee, 1998.

Li, W. K. W.: Macroecological patterns of phytoplankton in the northwestern North Atlantic Ocean, Nature 419, 154–157, 2002.

Montagnes, D. J. S., Berges, J. A., Harrison, P. J., and Taylor, F. J. R.: Estimating carbon, nitrogen, protein, and chlorophyll a from volume in marine phytoplankton, Limnol. Oceanogr., 39, 1044–1060, 1994.

Peters, R. H.: The ecological implications of body size, Cambridge University Press, Cambridge, 1983.

Raven, J. A. and Johnston, A. M.: Inorganic carbon acquisition mechanisms in marine phytoplankton and their implications for the use of other resources, Limnol. Oceanogr., 36, 1701–1714, 1991.

Riebesell, U., Wolf-Gladrow, D. A., and Smetacek, V.: Carbon dioxide limitation of marine phytoplankton growth rates, Nature, 361, 249–251, 1993.

Riebesell, U., Zondervan, I., Rost, B., Tortell, P.D., Zeebe, R., and Morel, F. M. M.: Reduced calcification of marine plankton in response of increased atmospheric CO_2, Nature, 407, 364–367, 2000.

Rost, B., Riebesell, U., Burkhardt, S., and Sültemeyer, D.: Carbon acquisition of bloom-forming marine phytoplankton, Limnol. Oceanogr., 48, 55–67, 2003.

Rost, B. and Riebesell, U.: Coccolithophores and the biological pump: responses to environmental changes, 99–127, In: Coccolithophores, From Molecular Processes to Global Impact, edited by: Thierstein, H. R. and Young, J. R., 2004.

Roy, R., Roy, L. N., Vogel, K. M., Portemoore, C., Pearson, T., Good, C. E., Millero, J., and Campbell, D. M.: The dissociation constants of carbonic acid in seawater at salinities 5 to 45 and temperatures 0 to 458C, Marine Chemistry, 44, 249–267, 1993.

Qiu, B. and Gao, K.: Effects of CO_2 enrichment on

the bloom-forming cyanobacterium *Microcystis aeruginosa* (Cyanophyceae): physiological responses and relationships with the availability of Dissolved Inorganic Carbon, J. Phycol., 38, 721–729, 2002.

Sciandra, A., Harlay, J., Lefèvre, D., Lemée, R., Rimmelin, P., Denis, M., and Gattuso, J.-P.: Response of the coccolithophorid *Emiliania huxleyi* to elevated pCO_2 under nitrate limitation, Marine Ecology Progress Series, 261, 111–122, 2003.

Schulz, K. G., Riebesel, L. U., Bellerby, R. G. J., Biswas, H., Meyerhöfer, M., Müller, M. N., Egge, J. K., Nejstgaard, J. C., Neill, C., Wohlers, J., and Zöllner, E.: Build-up and decline of organic matter during PeECE III, Biogeoscience Discuss., 4, 4539–4570, 2007.

Sheldon, R. W. and Parsons, T. R.: A practical manual on the use of the Coulter Counter in marine science, Coulter Electronic Sales Co., 1978.

Tortell, P. D., DiTullio, G. R., Sigman, D. M., and Morel, F. M. M.: CO_2 effects on taxonomic composition and nutrient utilization in an Equatorial Pacific phytoplankton assemblage, Marine Ecology-Progress Series, 236, 37–43, 2002.

Koroleff, F. and Grasshof, K.: Determination of nutrients, 125–188, in: Methods of seawater analyses, edited by: Grasshof, K., Erhardt, M., and Kremling, K., Verlag Chemie, Weinheim, 1983.

Sachs, L.: Angewandte Statistik, Springer Verlag Berlin Heidelberg New York, 1974.

Verity, P. G., Robertson, C. Y., Tronzo, C. R. Andrews, M. G., Nelson, J. R., and Sieracki, M. E.: Relationships between cell volume and the carbon and nitrogen content of marine photosynthetic nanoplankton, Limnol. Oceanogr., 37, 1434–1446, 1993.

Wolf-Gladrow, D. and Riebesell, U.: Diffusion and reactions in the vicinity of plankton: A refined model for inorganic carbon transport, Marine Chemistry, 59, 17–34, 1997.

Wolf-Gladrow, D., Riebesell, U., Burkhardt, S., and Bijma, J.: Direct effects of CO_2 concentration on growth and isotopic composition of marine plankton, Tellus, 51, 461–476, 1999.

Young, E. B. and Beardall, J.: Modulation of photosynthesis and inorganic carbon acquisition in a marine microalga by nitrogen, iron, and light availability, Canadian Journal Botany, 83, 917–928, 2005.

Zimmerman R. C., Kohrs D. G., Steller D. L., and Alberte, R. S.: Impacts of CO_2 enrichment on productivity and light requirements of eelgrass, Plant Physiology, 115, 599–607, 1997.